Electronic Supplementary Information

Quantifying the barrier for the movement of cyclobis(paraquat-*p*-phenylene) over the dication of monopyrrolotetrathiafulvalene

Rikke Kristensen,‡[a] Mathias S. Neumann,‡[a] Sissel S. Andersen,[a] Paul C. Stein,[a] Amar H. Flood[b] and Jan O. Jeppesen*[a]

[a] *Department of Physics, Chemistry and Pharmacy, University of Southern Denmark, Campusvej 55, DK-5230 Odense M, Denmark.*
E-mail: joj@sdu.dk; Tel: +45 65 50 25 87
[b] *Department of Chemistry, Indiana University, 800 E. Kirkwood Avenue Bloomington, IN 47405-7102, USA*
‡ Both authors contributed equally to this work.

(25 Pages)

Contents

Assigned ^{1}H NMR spectrum of 2•4PF$_6$

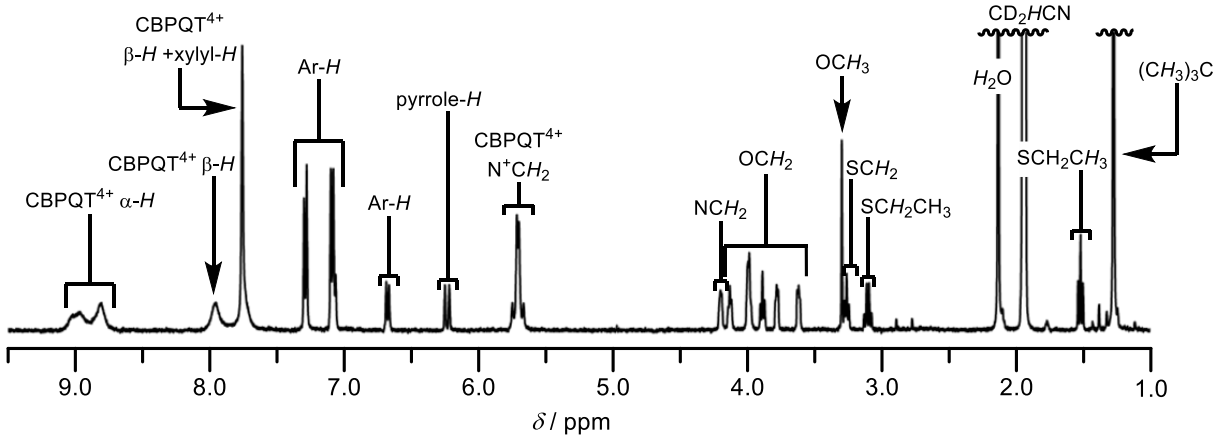

Fig. S1 Partial ^{1}H NMR spectrum (400 MHz, 298 K, CD_3CN) of the [2]rotaxane **2**•4PF_6 (*c* = 2 mM). The $(CH_3)_3C$, CD_2HCN and H_2O signals are not shown in their full height.

Synthesis of compound 9

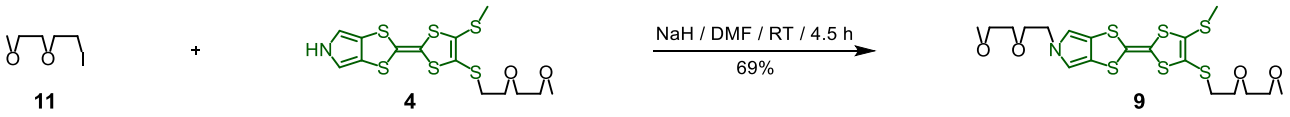

Scheme S1 Synthesis of the MPTTF derivative **9**.

Compounds **11**[S1] and **4**[S2] were synthesised according to literature procedures and compound **9** was synthesised as illustrated in Scheme S1. Initial deprotonation of the pyrrole *N*-H proton by NaH was followed by *N*-alkylation with the iodide **11** affording the MPTTF derivative **9** in 69% yield.

Binding study between the model compound 9 and CBPQT^{4+}

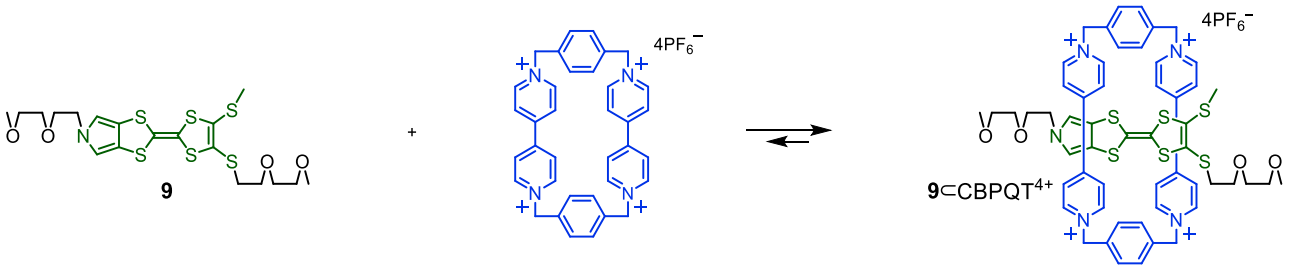

Scheme S2 Complexation between CBPQT^{4+} and the model compound **9** forming the [2]pseudorotaxane **9**⊂CBPQT^{4+}.

The binding constant K_a between the model compound **9** and CBPQT^{4+} and the related free energy ΔG^o for the complexation process were determined using the UV/Vis/NIR dilution method described by Nygaard *et al.*[S3] Mixing equimolar amounts of the MPTTF derivative **9** (yellow) with a solution of CBPQT•4PF$_6$ (colourless) in MeCN immediately resulted in a green-coloured solution as a result of the formation of a charge-transfer complex with an absorption band centered at 815 nm in the UV-Vis-NIR spectrum. Two independent starting solutions (2.4 mL) with an absolute concentration of 8.0×10^{-4} M were prepared and allowed to equilibrate at 298 K in the thermostated cell compartment of the spectrophotometer, before the absorbance A_m was measured. Subsequently, the solutions were repeatedly diluted to 5/6 of its initial concentration with MeCN, resulting in two series of 13 data points [$A^{-1/2}$, cA^{-1}] (Table S1).

Optical path length:	l = 1 cm	
CBPQT•4PF$_6$ in MeCN:	ε = 3.9 M^{-1} cm^{-1}	at λ = 815 nm
9 in MeCN:	ε = 2.5 M^{-1} cm^{-1}	at λ = 815 nm
Total background absorbance A_b:	ε = 6.4 M^{-1} cm^{-1}	at λ = 815 nm

Plotting cA^{-1} as a function of $A^{-1/2}$ afforded a straight line with a slope α of $(1/K_a\varepsilon l)^{1/2}$ and a y-intercept y_0 of $1/\varepsilon l$, where ε is the molar extinction coefficient and l is the optical path length. This linear plot gave a correlation coefficient of 0.998. The values for K_a and ε were obtained from the relationship $K_a = y_0/\alpha^2$ and the already shown relationship for y_0, respectively. The free energies of complexation $\Delta G°$ were obtained from the relationship $\Delta G° = -RT\ln K_a$, where R is the gas constant and T is the absolute temperature. The error of the binding constant (ΔK_a) is determined using the method described by Nygaard *et al.*[S3]

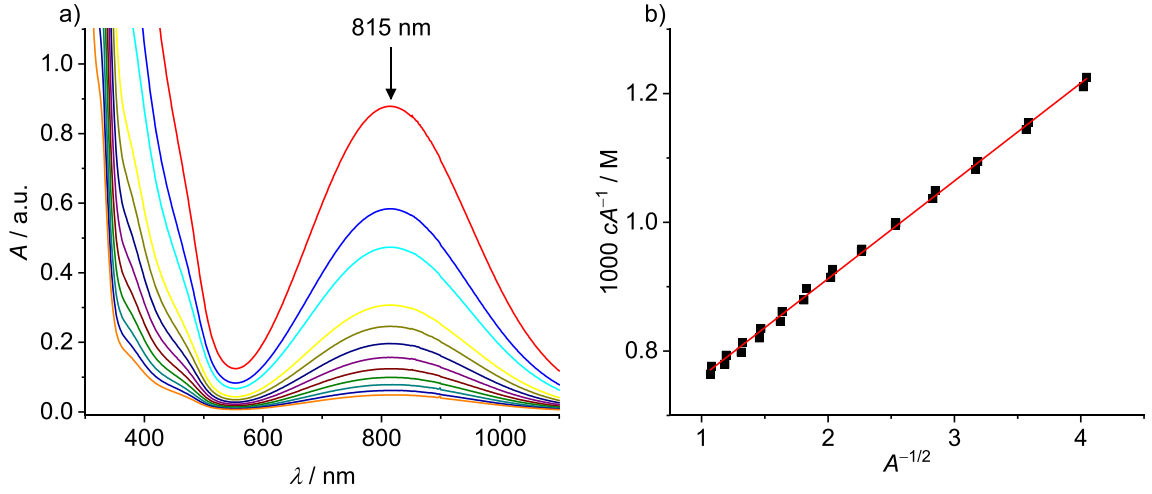

Fig. S2 a) UV-Vis-NIR spectra recorded of a 1:1 mixture of **9** and CBPQT^{4+} at 298 K in MeCN. b) Plot of 1000 cA^{-1} as a function of $A^{-1/2}$.

Table S1 The measured absorbance A_m for a 1:1 mixture of CBPQT•4PF_6 and **9** (MeCN, 298 K) at λ_{max} = 815 nm at different concentrations c, and the actual absorbance A obtained by subtracting the background absorbance A_b at 815 nm from the measured absorbance A_m (*i.e.* $A = A_m - A_b = A_m - 6.4\ M^{-1}cm^{-1} \times c \times l$)

c [× 10^{-3} M]	A_m	A	cA^{-1} [× 10^{-3} M]	$A^{-1/2}$
0.668	0.878	0.874	0.764	1.070
0.557	0.717	0.714	0.780	1.184
0.464	0.584	0.581	0.799	1.312
0.387	0.474	0.471	0.821	1.457
0.322	0.383	0.381	0.846	1.621
0.268	0.307	0.305	0.878	1.810
0.224	0.246	0.245	0.916	2.022
0.186	0.196	0.195	0.953	2.263
0.155	0.156	0.155	0.997	2.536
0.129	0.124	0.123	1.046	2.847
0.108	0.099	0.099	1.096	3.185
0.090	0.078	0.078	1.157	3.585
0.075	0.062	0.061	1.227	4.044
0.668	0.865	0.860	0.776	1.078
0.557	0.705	0.702	0.794	1.194
0.464	0.573	0.570	0.814	1.324
0.387	0.465	0.463	0.836	1.470
0.322	0.376	0.374	0.861	1.635
0.268	0.301	0.299	0.896	1.828
0.224	0.243	0.241	0.928	2.035
0.186	0.196	0.195	0.956	2.267
0.155	0.157	0.156	0.993	2.531
0.129	0.126	0.125	1.033	2.830
0.108	0.100	0.100	1.083	3.167
0.090	0.079	0.079	1.145	3.567
0.075	0.062	0.062	1.212	4.020

Binding study between the semidumbbell 1 and CBPQT^{4+}

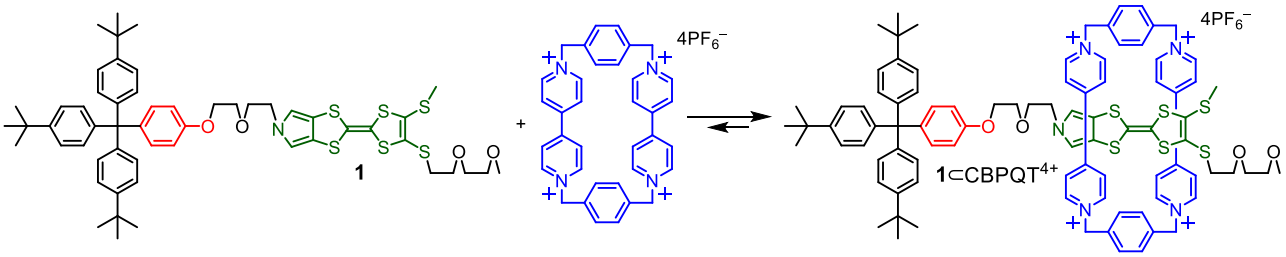

Scheme S3 Complexation between CBPQT^{4+} and the semidumbbell **1** forming the [2]pseudorotaxane **1**⊂CBPQT^{4+}.

The binding constant K_a between the semidumbbell **1** and CBPQT^{4+} and the related free energy ΔG^o for the complexation process were determined using the UV-Vis-NIR dilution method described by Nygaard *et al.*[S3] As the complexation process is slow exchange, the stock solutions were made one day in advance by mixing equimolar amounts of the semidumbbell **1** (yellow) with a solution of CBPQT•4PF$_6$ (colorless) in MeCN. Overnight the stock solutions turned green as a result of the formation of a charge-transfer complex with an absorption band centered at 816 nm in the UV-Vis-NIR spectrum. Appropriate dilutions of the two independent stock solutions produced samples with absolute concentrations in the range of 6.7×10^{-5} to 8.0×10^{-4} M which again was left overnight to equilibrate. The samples were allowed to equilibrate at 298 K in the thermostated cell compartment of the spectrophotometer, before the absorbance A_m was measured which resulted in two series of 15 data points [$1A^{-1/2}$, cA^{-1}] (Table S2).

Optical path length:	l = 1 cm	
CBPQT•4PF$_6$ in MeCN:	ε = 4.1 M^{-1} cm^{-1}	at λ = 816 nm
1 in MeCN:	ε = 21 M^{-1} cm^{-1}	at λ = 816 nm
Total background absorbance A_b:	ε = 25 M^{-1} cm^{-1}	at λ = 816 nm

Plotting cA^{-1} as a function of $A^{-1/2}$ afforded a straight line with a slope α of $(1/K_a\varepsilon l)^{1/2}$ and a y-intercept y_0 of $1/\varepsilon l$, where ε is the molar extinction coefficient and l is the optical path length. This linear plot gave a correlation coefficient of 0.980. The values for K_a and ε were obtained from the relationship $K_a = y_0/\alpha^2$ and the already shown relationship for y_0, respectively. The free energies of complexation $\Delta G°$ were obtained from the relationship $\Delta G° = -RT\ln K_a$, where R is the gas constant and T is the absolute temperature. The error of the binding constant (ΔK_a) is determined using the method described by Nygaard *et al.*[S3]

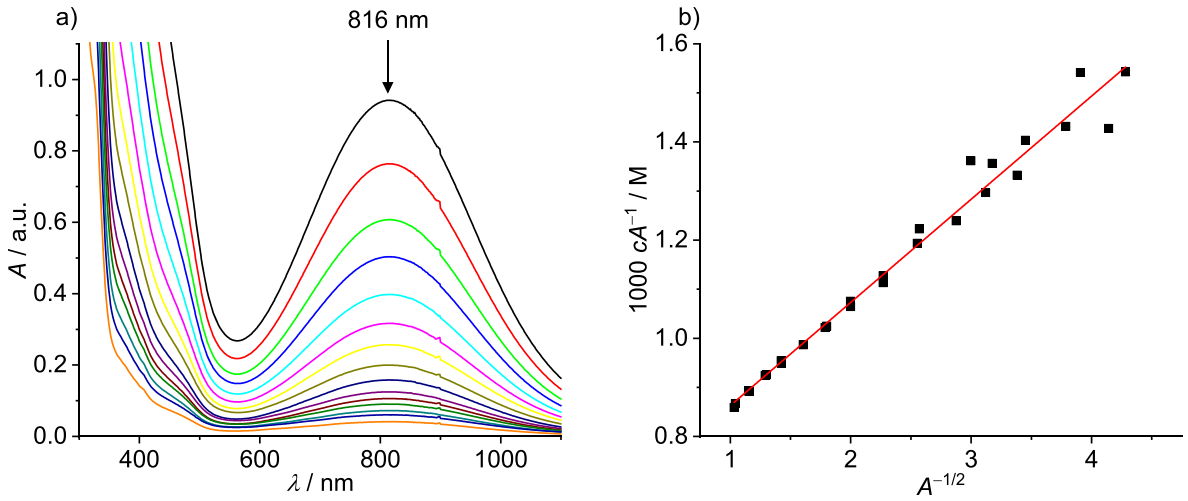

Fig. S3 a) UV-Vis-NIR spectra recorded of a 1:1 mixture of **1** and CBPQT^{4+} at 298 K in MeCN. b) Plot of 1000 cA^{-1} as a function of $A^{-1/2}$.

Table S2 The measured absorbance A_m for a 1:1 mixture of CBPQT•4PF_6 and **1** (MeCN, 298 K) at λ_{max} = 816 nm at different concentrations c, and the actual absorbance A obtained by subtracting the background absorbance A_b at 816 nM from the measured absorbance A_m (*i.e.* $A = A_m - A_b = A_m - 25\ M^{-1}\ cm^{-1} \times c \times l$)

c [× 10^{-3} M]	A_m	A	cA^{-1} [× 10^{-3} M]	$A^{-1/2}$
0.799	0.942	0.922	0.867	1.041
0.666	0.764	0.747	0.892	1.157
0.549	0.607	0.594	0.925	1.298
0.466	0.503	0.492	0.948	1.426
0.383	0.398	0.388	0.987	1.605
0.316	0.317	0.309	1.024	1.800
0.266	0.257	0.250	1.063	1.999
0.216	0.200	0.194	1.111	2.268
0.183	0.158	0.153	1.192	2.553
0.150	0.125	0.121	1.241	2.876
0.133	0.106	0.103	1.295	3.121
0.117	0.090	0.087	1.338	3.382
0.100	0.072	0.070	1.434	3.786
0.083	0.060	0.058	1.423	4.141
0.067	0.041	0.039	1.702	5.040
0.808	0.961	0.941	0.859	1.031
0.674	0.771	0.755	0.893	1.151
0.556	0.615	0.601	0.925	1.290
0.471	0.506	0.494	0.953	1.422
0.387	0.403	0.393	0.984	1.595
0.320	0.321	0.313	1.022	1.787
0.269	0.257	0.251	1.074	1.998
0.219	0.200	0.194	1.128	2.269
0.185	0.156	0.151	1.222	2.570
0.152	0.115	0.111	1.366	2.998
0.135	0.103	0.099	1.360	3.174
0.118	0.087	0.084	1.405	3.451
0.101	0.068	0.066	1.541	3.906
0.084	0.057	0.055	1.539	4.281
0.067	0.039	0.038	1.786	5.164

Illustration of the redox processes taking place upon electrochemical oxidation of 2^{4+} and $1\subset CBPQT^{4+}$

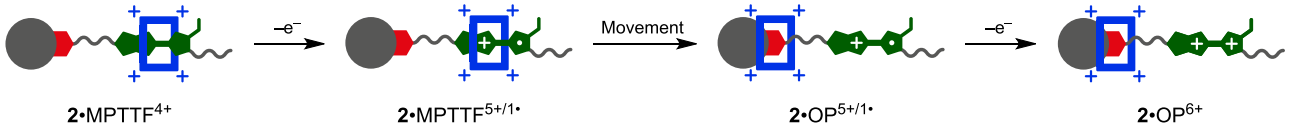

Scheme S4 Cartoon representation of the redox processes to produce **2**•OP^{6+} upon electrochemical oxidation of **2**•$MPTTF^{4+}$.

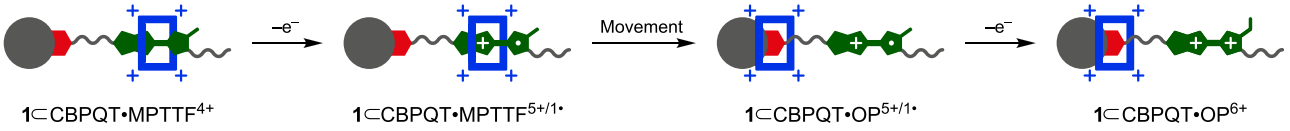

Scheme S5 Cartoon representation of the redox processes to produce **1**⊂CBPQT•OP^{6+} upon electrochemical oxidation of **1**⊂CBPQT•$MPTTF^{4+}$.

Kinetic investigations of 1⊂CBPQT•MPTTF^{4+}

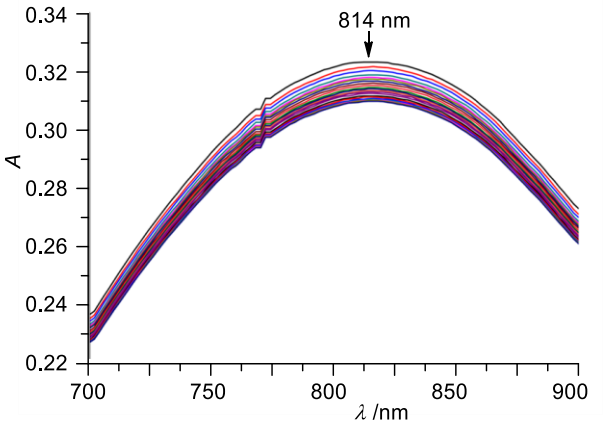

Fig. S4 UV-Vis-NIR absorption spectra of the [2]pseudorotaxane **1**⊂CBPQT•MPTTF^{4+} in MeCN at 298 K. The top spectrum is recorded as soon as possible after heating the solution to 298 K and the subsequent spectra are recorded every 10 s.

Assigned ^{1}H NMR spectrum of 1⊂CBPQT^{4+}

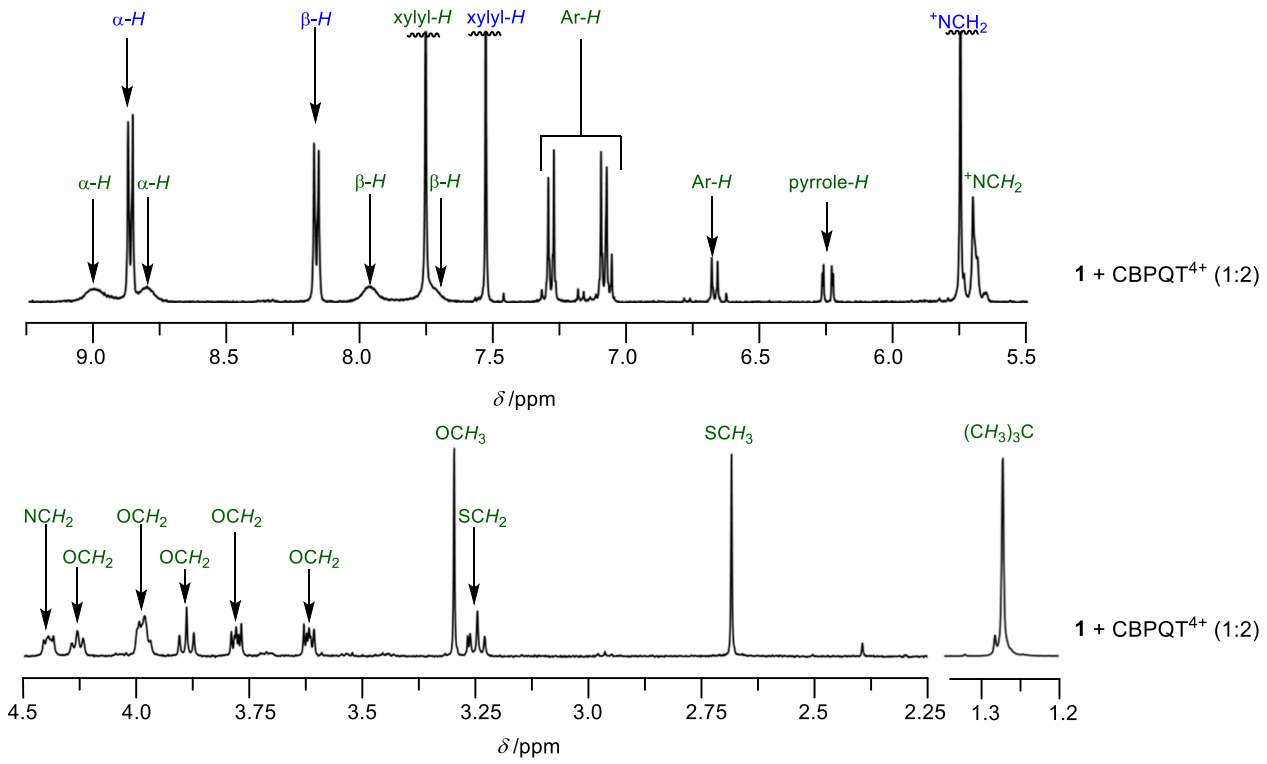

Fig. S5 Partial ^{1}H NMR spectrum (400 MHz, 298 K, CD_3CN, 2 mM) recorded of an equilibrated 1:2 mixture of **1** and CBPQT^{4+}, where assignments in green are associated with the [2]pseudorotaxane **1**⊂CBPQT^{4+} and assignments in blue are associated with the uncomplexed CBPQT^{4+}. The region from 1.20 to 1.32 is scaled down.

Oxidation experiments on 1⊂CBPQT^{4+} and 2^{4+}

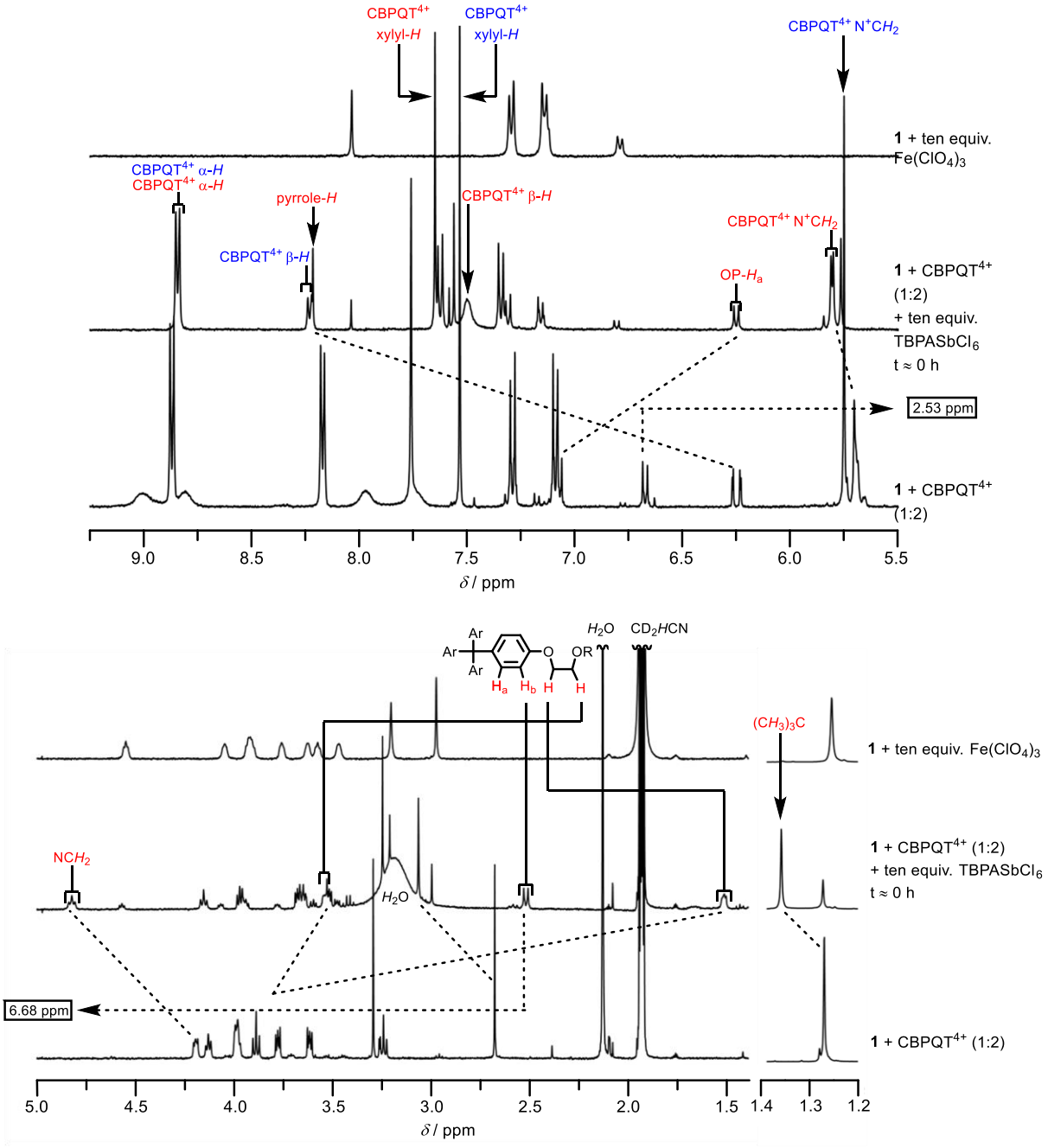

Fig. S6 Partial ^{1}H NMR spectra (400 MHz, 298 K, CD_3CN, 2 mM) of **1** and CBPQT^{4+} (1:2 ratio), **1** and CBPQT^{4+} (1:2 ratio) + ten equiv. $TBPASbCl_6$ as soon as possible after mixing and **1** with ten equiv. $Fe(ClO_4)_3$. The areas omitted have no signals. The area from 1.2 to 1.4 ppm is scaled down to clarify the separation and height of the two $(CH_3)_3C$ signals. The CD_2HCN signal as well as the H_2O signals are not shown in their full height. Blue assignments are from free CBPQT^{4+} and red assignments are from **1**⊂CBPQT•OP^{6+}. Only distinct signals are assigned.

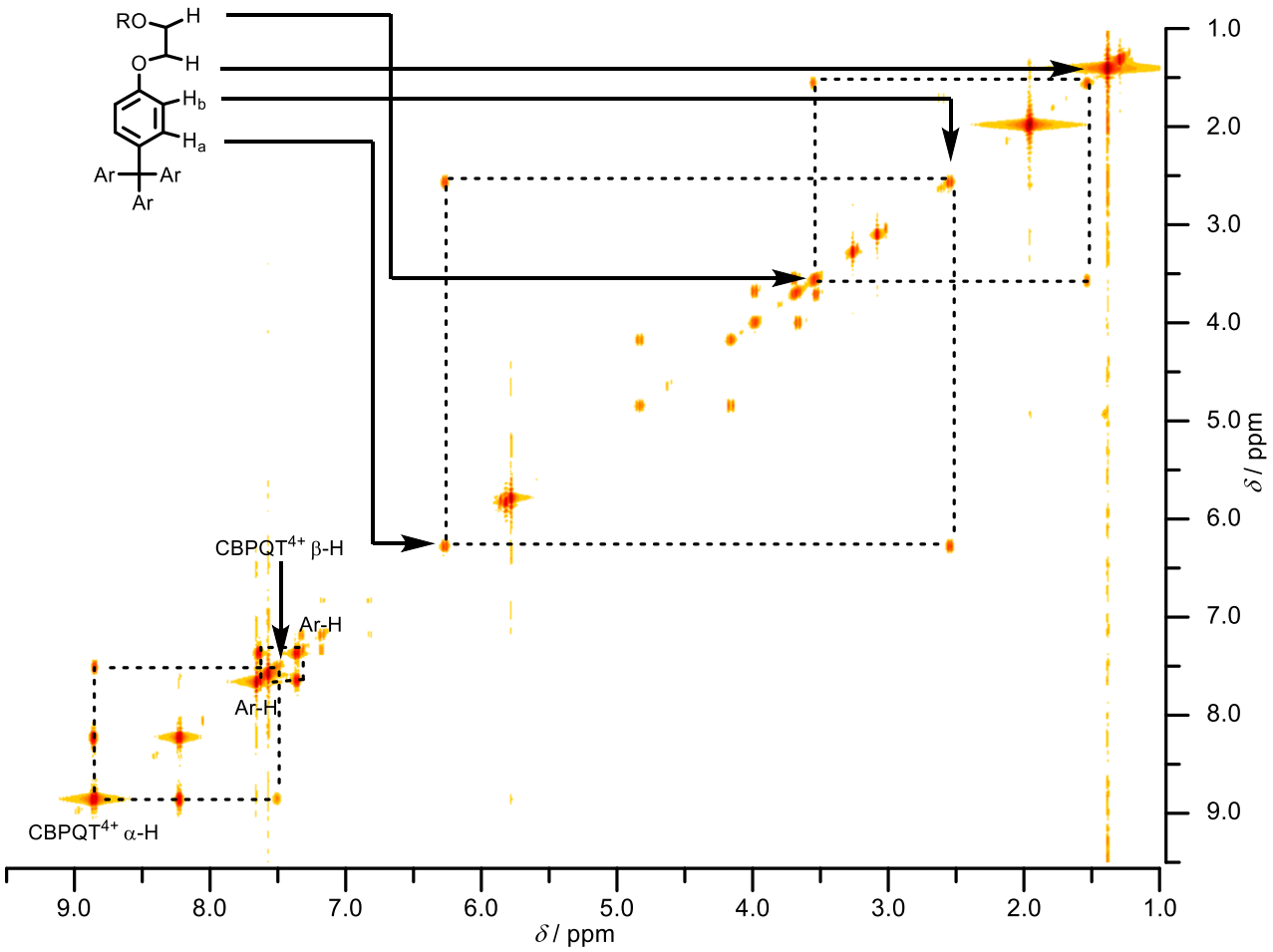

Fig. S7 COSY spectrum (400 MHz, 298) recorded as fast as possible after addition of ten equiv. $TBPASbCl_6$ to a solution of **1**⊂$CBPQT^{4+}$ in CD_3CN (*c* = 2 mM) resulting in **1**⊂CBPQT•OP^{6+}. The structure shown is the part of the stopper which is encircled by $CBPQT^{4+}$.

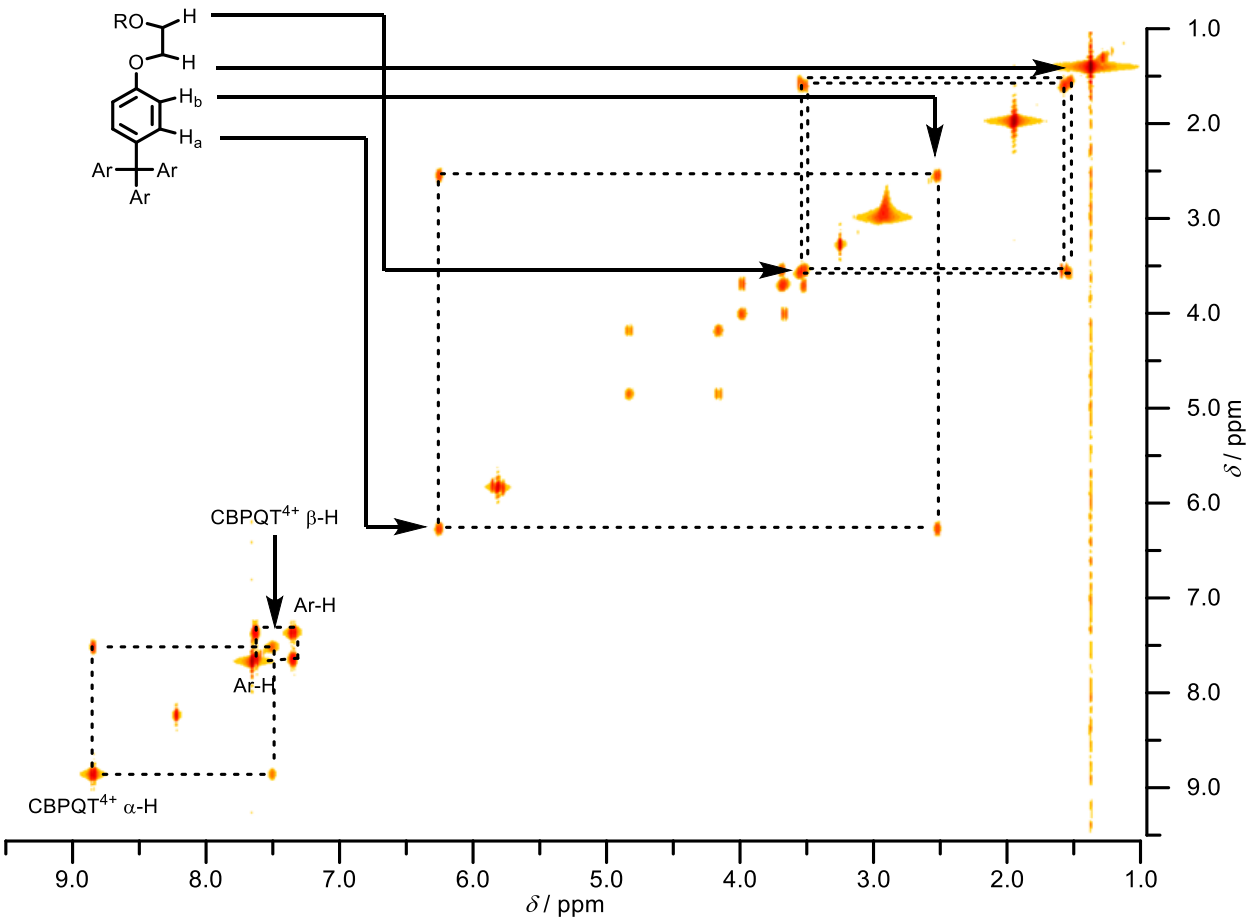

Fig. S8 COSY spectrum (400 MHz, 298 K) as fast as possible after addition of ten equiv. $TBPASbCl_6$ to a solution in CD_3CN of $\mathbf{2}^{4+}$ (c = 2 mM) resulting in $\mathbf{2}\bullet OP^{6+}$. The structure shown is the part of the stopper encircled by $CBPQT^{4+}$.

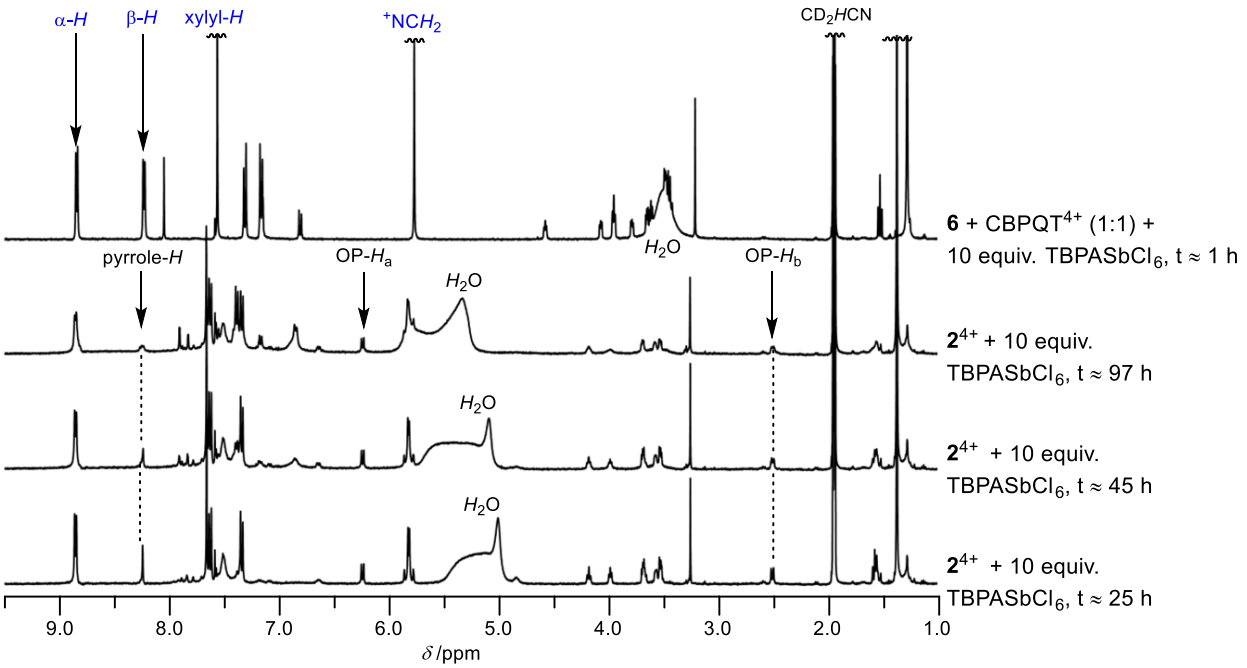

Fig. S9 Partial ^{1}H NMR spectra (400 MHz, 298 K, CD_3CN) of $\mathbf{2}^{4+}$ (2 mM) + tenequiv. $TBPASbCl_6$ recorded 25, 45 and 97 h after mixing and of **6** + $CBPQT^{4+}$ (1:1, 2 mM) + ten equiv. $TBPASbCl_6$. The $(CH_3)_3C$, CD_2HCN, $^+NCH_2$ and xylyl-*H* are not shown in full height. The blue assignments are from free $CBPQT^{4+}$ and the black assignments are from $\mathbf{2}^{4+}$.

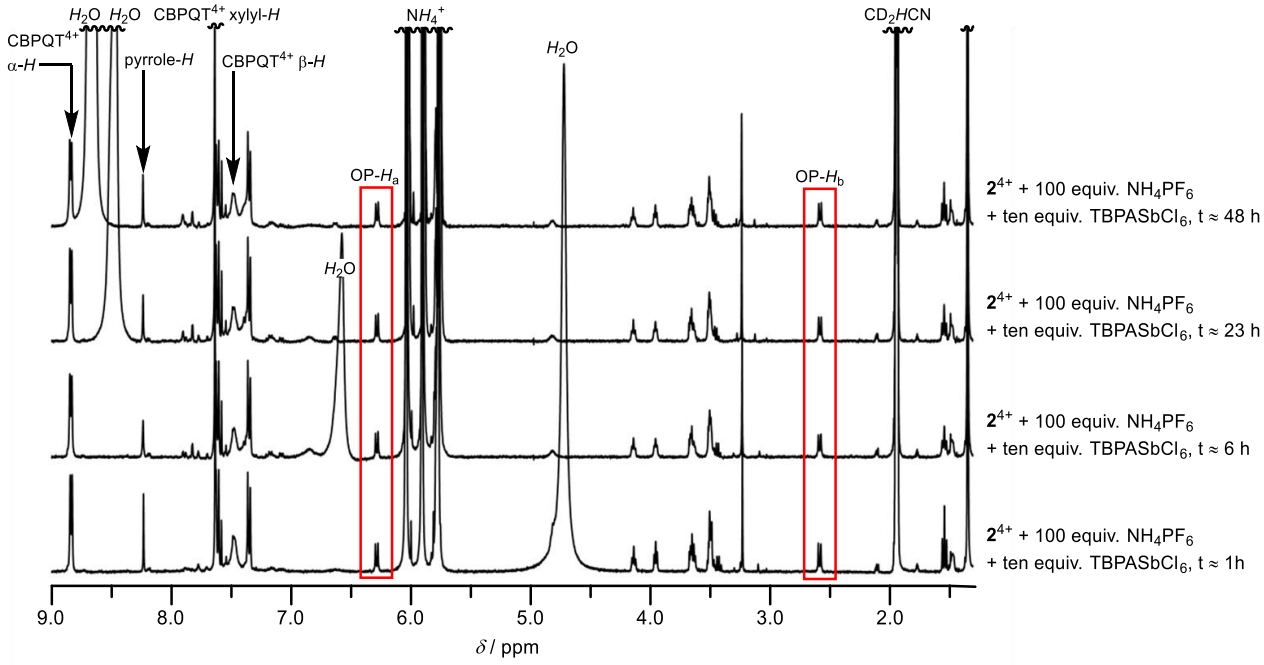

Fig. S10 Partial ^{1}H NMR spectra (400 MHz, 298 K, CD_3CN) of $\mathbf{2}^{4+}$ (*c* = 2 mM with 0.2 M NH_4PF_6) + ten equiv. $TBPASbCl_6$ recorded 1, 6, 23 and 48 h after mixing. The $(CH_3)_3C$, CD_2HCN, N^+CH_2, NH_4^+ and xylyl-*H* from free $CBPQT^{4+}$ signals are not shown in their full height. The assigned resonances are all from $\mathbf{2}^{6+}$ or residual solvent peaks. The complete assignment can be found in Fig. S11.

It is evident that all four spectra in Fig. S10 are almost identical. By integrating the signals from the phenylene group in the bulky stopper unit and comparing the integrals to those of the tetramethylsilane(TMS) signal, it becomes clear that they are not changing over time. This observation indicates that **2**$^{6+}$ is stable for more than 48 h in the presence of 100 equiv. NH_4PF_6 at 298 K and that CBPQT^{4+} does not deslip (Scheme S6).

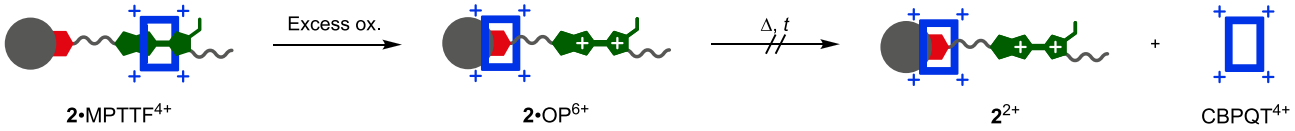

Scheme S6 Movement mechanism in the [2]rotaxane **2**•MPTTF^{4+} after addition of ten equiv. $TBPASbCl_6$.

Determining the size of the MPTTF^{2+}/SMe/TDEG barrier in 1⊂CBPQT^{6+}

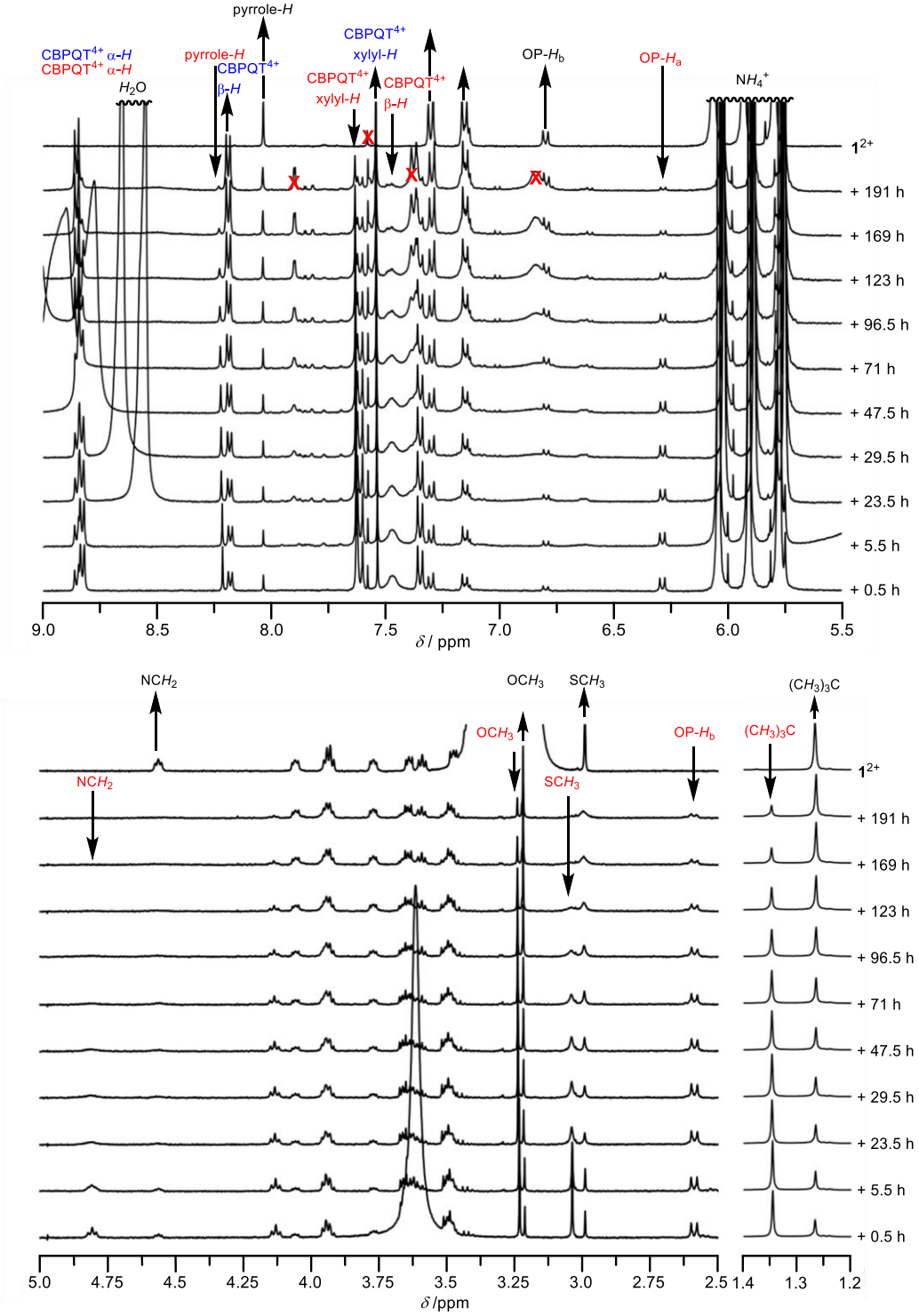

Fig. S11 Partial ^{1}H NMR spectra (400 MHz, 298 K) of **1**⊂CBPQT^{4+} produced by mixing **1** (2 mM) and CBPQT^{4+} (4 mM) in CD_3CN and then allowed to equilibrate for 10 h in the presence of NH_4PF_6 (0.2 M) followed by oxidation with ten equiv. $TBPASbCl_6$. The spectra are recorded at different delay times after addition of $TBPASbCl_6$. The areas omitted have no signals or only contain the residual solvent peak. The area from 1.2 to 1.4 ppm is scaled down to clarify the separation and height of the two $(CH_3)_3C$ signals. The NH_4 signal as well as the H_2O signal are not shown in their full height. Assignments in blue are from free CBPQT^{4+}, assignments in red are from **1**⊂CBPQT•OP^{6+} and assignments in black are from **1**$^{2+}$.

The stability of **1**⊂CBPQT^{6+} over time is poor. To keep it stable all experiments are performed with the presence of 0.2 M NH_4PF_6, which is found to increase the stability of oxidised MPTTF.

Because it is possible to follow the movement of CBPQT^{4+} from the position around the OP station in **1**⊂CBPQT•OP^{6+} and over the MPTTF^{2+}/SMe/TDEG barrier, it is possible to qualitatively determine the size of the combined MPTTF^{2+}/SMe/TDEG barrier. The experiments shown in Fig. S11 were repeated, but spectra were recorded more frequently (every hour for three days) to get enough data points to calculate the rate of CBPQT^{4+} deslipping from **1**⊂CBPQT^{6+}. The experiments were repeated at 294, 303, 308, 313 and 323 K, and the first ^{1}H NMR spectrum was recorded as soon as possible after addition of ten equiv. $TBPASbCl_6$ to an equilibrated 1:2 mixture of the semidumbbell **1** and CBPQT^{4+} in CD_3CN with NH_4PF_6 (0.2 M). By treating the deslipping as a first order process, it is possible to use first order kinetics (ln*I* as a function of time, *t*, Fig. S12) to determine the rate constant k_d for the movement of CBPQT^{4+}.

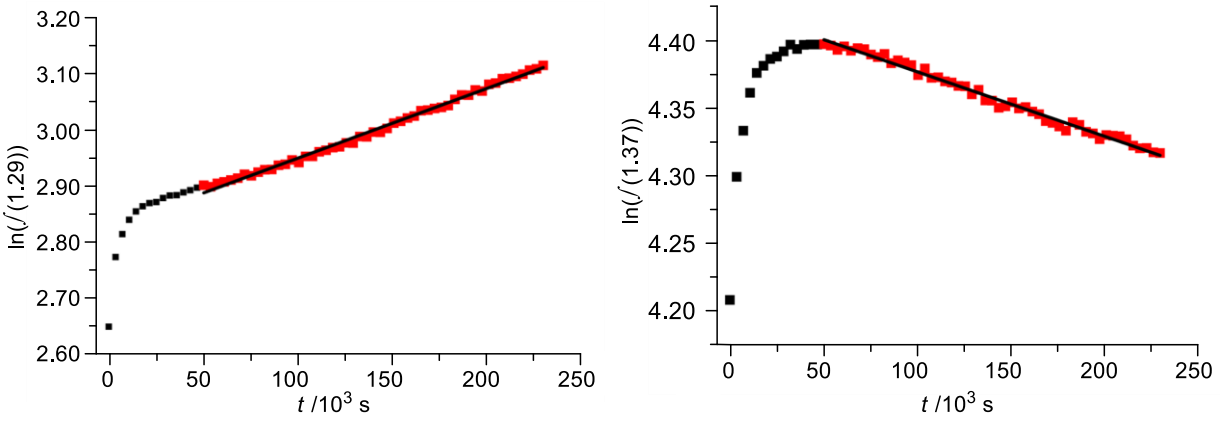

Fig. S12 The natural logarithm of the integral of the singlets (294 K) resonating at 1.29 and 1.37 ppm, respectively, as a function of time. The red data points are used to make a linear regression, from which the slope and thereby the rate constant of CBPQT^{4+} deslipping over the MPTTF^{2+}/SMe/TDEG barrier can be found.

Table S3 Rate constants, k_d, energies of activation, $\Delta G^{\ddagger}_d$ and correlation coefficients, R^2, from CBPQT^{4+} deslipping over the MPTTF^{2+}/SMe/TDEG barrier measured at 294 K in CD_3CN (0.2 M NH_4PF_6) by following the process with ^{1}H NMR spectroscopy (500 MHz), using different signals as probes. Errors are calculated based on Koumura *et al.*[S4] with ΔT = 0.2 K and ΔI = 0.05%

Assignment	δ / ppm	k_d / s^{-1}	$\Delta G^{\ddagger}_d$ / kcal mol^{-1}	R^2
2^{2+}	1.29	$1.24 \times 10^{-6} \pm 2.78 \times 10^{-10}$	25.17 ± 0.02	0.995
2⊂CBPQT•OP^{6+}	1.37	$4.73 \times 10^{-7} \pm 7.12 \times 10^{-11}$	25.73 ± 0.02	0.989
2^{2+}	3.21	$1.62 \times 10^{-6} \pm 3.67 \times 10^{-9}$	25.02 ± 0.02	0.973
2⊂CBPQT•OP^{6+}	3.24	$3.98 \times 10^{-7} \pm 7.59 \times 10^{-10}$	25.83 ± 0.02	0.977
CBPQT^{4+}	7.54	$3.71 \times 10^{-7} \pm 1.87 \times 10^{-10}$	25.88 ± 0.02	0.979

Table S4 Rate constants, k_d, energies of activation, $\Delta G^{\ddagger}_d$ and correlation coefficients, R^2, from $CBPQT^{4+}$ deslipping over the $MPTTF^{2+}$/SMe/TDEG barrier measured at 303 K in CD_3CN (0.2 M NH_4PF_6) by following the process with ^1H NMR spectroscopy (500 MHz), using different signals as probes. Errors are calculated based on Koumura *et al.*[S4] with ΔT = 0.2 K and ΔI = 0.05%

Assignment	δ / ppm	k_d / s^{-1}	$\Delta G^{\ddagger}_d$ / kcal mol^{-1}	R^2
$\mathbf{2}^{2+}$	1.29	$3.12 \times 10^{-6} \pm 4.14 \times 10^{-10}$	25.40 ± 0.02	0.982
$\mathbf{2}\subset CBPQT{\bullet}OP^{6+}$	1.37	$9.40 \times 10^{-7} \pm 1.22 \times 10^{-10}$	26.13 ± 0.02	0.969
$\mathbf{2}^{2+}$	3.21	$5.56 \times 10^{-6} \pm 7.67 \times 10^{-9}$	25.06 ± 0.02	0.978
$\mathbf{2}\subset CBPQT{\bullet}OP^{6+}$	3.24	$8.20 \times 10^{-7} \pm 1.29 \times 10^{-9}$	26.21 ± 0.02	0.942
$CBPQT^{4+}$	7.54	$8.31 \times 10^{-7} \pm 2.62 \times 10^{-10}$	26.20 ± 0.02	0.943

Table S5 Rate constants, k_d, energies of activation, $\Delta G^{\ddagger}_d$ and correlation coefficients, R^2, from $CBPQT^{4+}$ deslipping over the $MPTTF^{2+}$/SMe/TDEG barrier measured at 308 K in CD_3CN (0.2 M NH_4PF_6) by following the process with ^1H NMR spectroscopy (500 MHz), using different signals as probes. Errors are calculated based on Koumura *et al.*[S4] with ΔT = 0.2 K and ΔI = 0.05%

Assignment	δ / ppm	k_d / s^{-1}	$\Delta G^{\ddagger}_d$ / kcal mol^{-1}	R^2
$\mathbf{2}^{2+}$	1.29	$3.47 \times 10^{-6} \pm 1.64 \times 10^{-9}$	25.77 ± 0.02	0.998
$\mathbf{2}\subset CBPQT{\bullet}OP^{6+}$	1.37	$1.08 \times 10^{-6} \pm 6.94 \times 10^{-10}$	26.48 ± 0.02	0.957
$\mathbf{2}^{2+}$	3.21	$5.51 \times 10^{-6} \pm 2.23 \times 10^{-8}$	25.48 ± 0.02	0.978
$\mathbf{2}\subset CBPQT{\bullet}OP^{6+}$	3.24	$1.24 \times 10^{-6} \pm 7.01 \times 10^{-9}$	26.40 ± 0.02	0.956
$CBPQT^{4+}$	7.54	$1.67 \times 10^{-6} \pm 1.21 \times 10^{-9}$	26.22 ± 0.02	0.985

Table S6 Rate constants, k_d, energies of activation, $\Delta G^{\ddagger}_d$ and correlation coefficients, R^2, from $CBPQT^{4+}$ deslipping over the $MPTTF^{2+}$/SMe/TDEG barrier measured at 313 K in CD_3CN (0.2 M NH_4PF_6) by following the process with ^1H NMR spectroscopy (500 MHz), using different signals as probes. Errors are calculated based on Koumura *et al.*[S4] with ΔT = 0.2 K and ΔI = 0.05%

Assignment	δ / ppm	k_d / s^{-1}	$\Delta G^{\ddagger}_d$ / kcal mol^{-1}	R^2
$\mathbf{2}^{2+}$	1.29	$6.23 \times 10^{-6} \pm 7.67 \times 10^{-10}$	25.83 ± 0.02	0.995
$\mathbf{2}\subset CBPQT{\bullet}OP^{6+}$	1.37	$2.14 \times 10^{-6} \pm 2.89 \times 10^{-10}$	26.50 ± 0.02	0.961
$\mathbf{2}^{2+}$	3.21	$1.02 \times 10^{-5} \pm 1.20 \times 10^{-8}$	25.53 ± 0.02	0.990
$\mathbf{2}\subset CBPQT{\bullet}OP^{6+}$	3.24	$2.36 \times 10^{-6} \pm 3.18 \times 10^{-9}$	26.43 ± 0.02	0.972
$CBPQT^{4+}$	7.54	$2.53 \times 10^{-6} \pm 5.55 \times 10^{-10}$	26.39 ± 0.02	0.986

Table S7 Rate constants, k_d, energies of activation, $\Delta G^{\ddagger}_d$ and correlation coefficients, R^2, from $CBPQT^{4+}$ deslipping over the $MPTTF^{2+}$/SMe/TDEG barrier measured at 323 K in CD_3CN (0.2 M NH_4PF_6) by following the process with ^1H NMR spectroscopy (500 MHz), using different signals as probes. Errors are calculated based on Koumura *et al.*[S4] with ΔT = 0.2 K and ΔI = 0.05%

Assignment	δ / ppm	k_d / s^{-1}	$\Delta G^{\ddagger}_d$ / kcal mol^{-1}	R^2
$\mathbf{2}^{2+}$	1.29	$1.19 \times 10^{-5} \pm 1.88 \times 10^{-9}$	26.26 ± 0.02	0.901
$\mathbf{2}\subset CBPQT\bullet OP^{6+}$	1.37	$9.20 \times 10^{-6} \pm 1.47 \times 10^{-9}$	26.43 ± 0.02	0.931
$\mathbf{2}^{2+}$	3.21	$1.19 \times 10^{-5} \pm 3.10 \times 10^{-8}$	26.26 ± 0.02	0.879
$\mathbf{2}\subset CBPQT\bullet OP^{6+}$	3.24	$8.90 \times 10^{-6} \pm 1.60 \times 10^{-8}$	26.45 ± 0.02	0.872
$CBPQT^{4+}$	7.54	$9.09 \times 10^{-6} \pm 2.04 \times 10^{-9}$	26.43 ± 0.02	0.960

An average value of all five results (Table S3–S7) was used to calculate the final rate constants for $CBPQT^{4+}$ deslipping over the $MPTTF^{2+}$/SMe/TDEG barrier The results obtained at the five different temperatures are listed in Table S8.

Table S8 Average rate constants and $\Delta G^{\ddagger}$ values from $CBPQT^{4+}$ deslipping over the $MPTTF^{2+}$/SMe/TDEG barrier measured at different temperatures in CD_3CN (0.2 M NH_4PF_6) by following the process with ^1H NMR spectroscopy (500 MHz). Errors are calculated based on Koumura et al[S4] with ΔT = 0.2 K and ΔI = 0.05%

T / K	n	k_d / s^{-1}	$\Delta G^{\ddagger}_d$ / kcal mol^{-1}
294	51	$8.20 \times 10^{-7} \pm 9.93 \times 10^{-10}$	25.53 ± 0.02
303	45	$2.25 \times 10^{-6} \pm 1.95 \times 10^{-9}$	25.80 ± 0.02
308	24	$2.59 \times 10^{-6} \pm 6.57 \times 10^{-9}$	26.07 ± 0.02
313	22	$4.69 \times 10^{-6} \pm 3.36 \times 10^{-9}$	26.14 ± 0.02
323	8	$1.02 \times 10^{-5} \pm 1.05 \times 10^{-8}$	26.37 ± 0.02

By plotting the derived activation energies ($\Delta G^{\ddagger}_{d}$) as a function of temperature (T), it is possible to determine the enthalpy ($\Delta H^{\ddagger}_{d}$) and the entropy ($\Delta S^{\ddagger}_{d}$) according to the equation $\Delta G^{\ddagger}_{d} = \Delta H^{\ddagger}_{d} - T \times \Delta S^{\ddagger}_{d}$. The plot is shown in Fig. S13 and the kinetic parameters are summarized in Table S9.

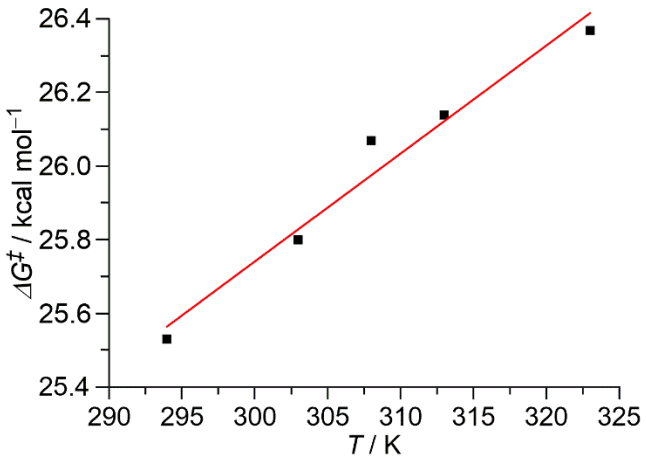

Fig. S13 The average activation energy ($\Delta G^{\ddagger}_{d}$) plotted against the temperature (T) in order to find the enthalpy ($\Delta H^{\ddagger}_{d}$) and the entropy ($\Delta S^{\ddagger}_{d}$). The slope and intercept of the linear regression give the values $-\Delta S^{\ddagger}_{d}$ and $\Delta H^{\ddagger}_{d}$, respectively from the equation $\Delta G^{\ddagger}_{d} = \Delta H^{\ddagger}_{d} - T \times \Delta S^{\ddagger}_{d}$.

Table S9 Kinetic parameters for the movement of $CBPQT^{4+}$ from the OP station over the $MPTTF^{2+}$/SMe/TDEG barrier in $\mathbf{2}^{2+}$ obtained by ^{1}H NMR spectroscopy (500 MHz, CD_3CN, 0.2 M NH_4PF_6) at 298 K

R^2	$\Delta G^{\ddagger}_{d}$ / kcal mol^{-1} [a]	$\Delta H^{\ddagger}_{d}$ / kcal mol^{-1} [a]	$\Delta S^{\ddagger}_{d}$ / cal mol^{-1} K^{-1} [a]
0.968	25.7 ± 0.1	15.5 ± 5.2	–33.9 ± 16.8

[a] Errors are calculated using Koumura *et al.*[S4] with ΔK = 0.2 K.

^{1}H NMR and ^{13}C NMR spectra of all compounds

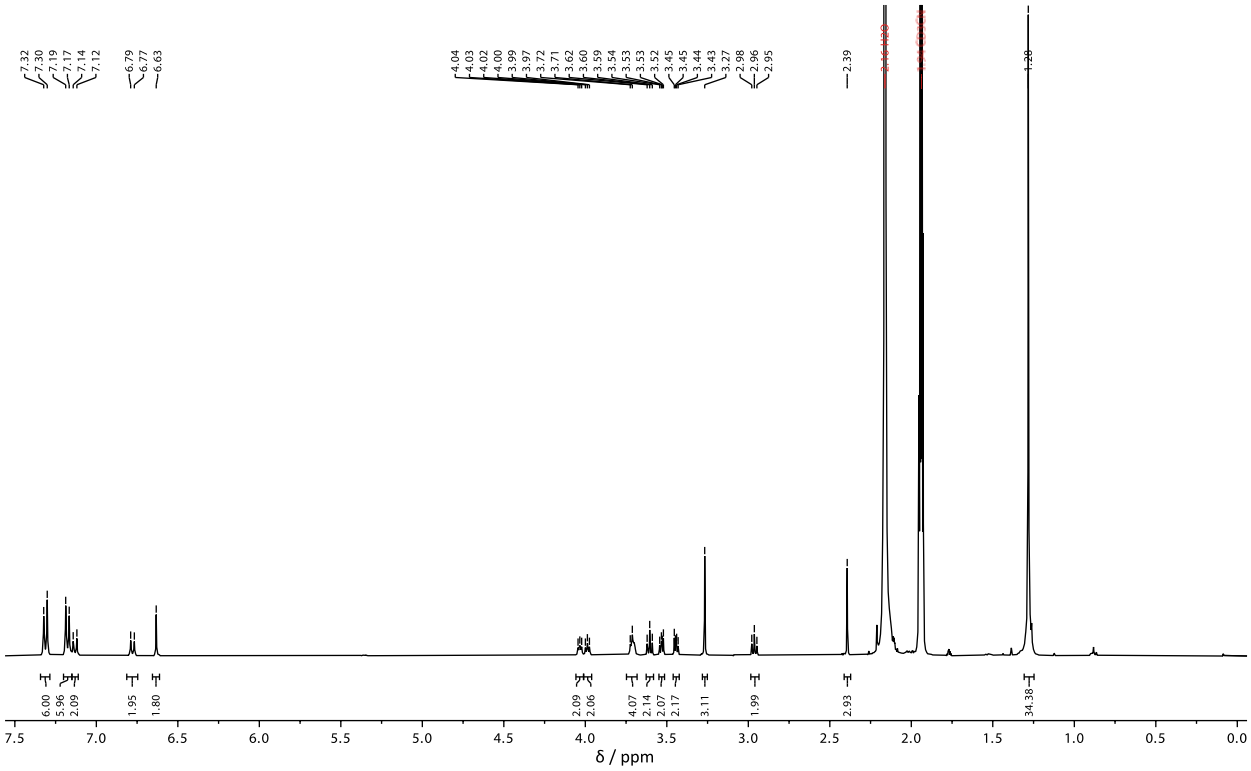

Fig. S14 ^{1}H NMR spectrum (400 MHz, 298K, CD_3CN) of the semidumbbell **1**.

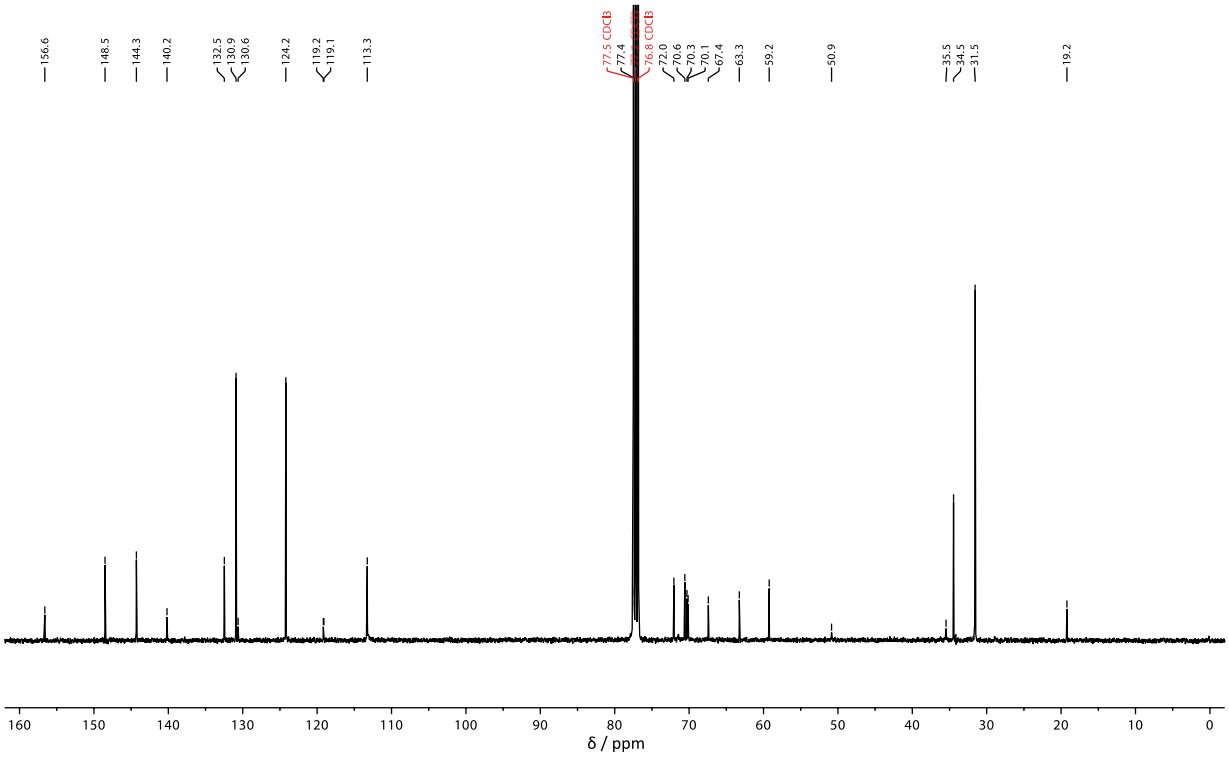

Fig. S15 ^{13}C NMR spectrum (100 MHz, 298K, $CDCl_3$) of the semidumbbell **1**.

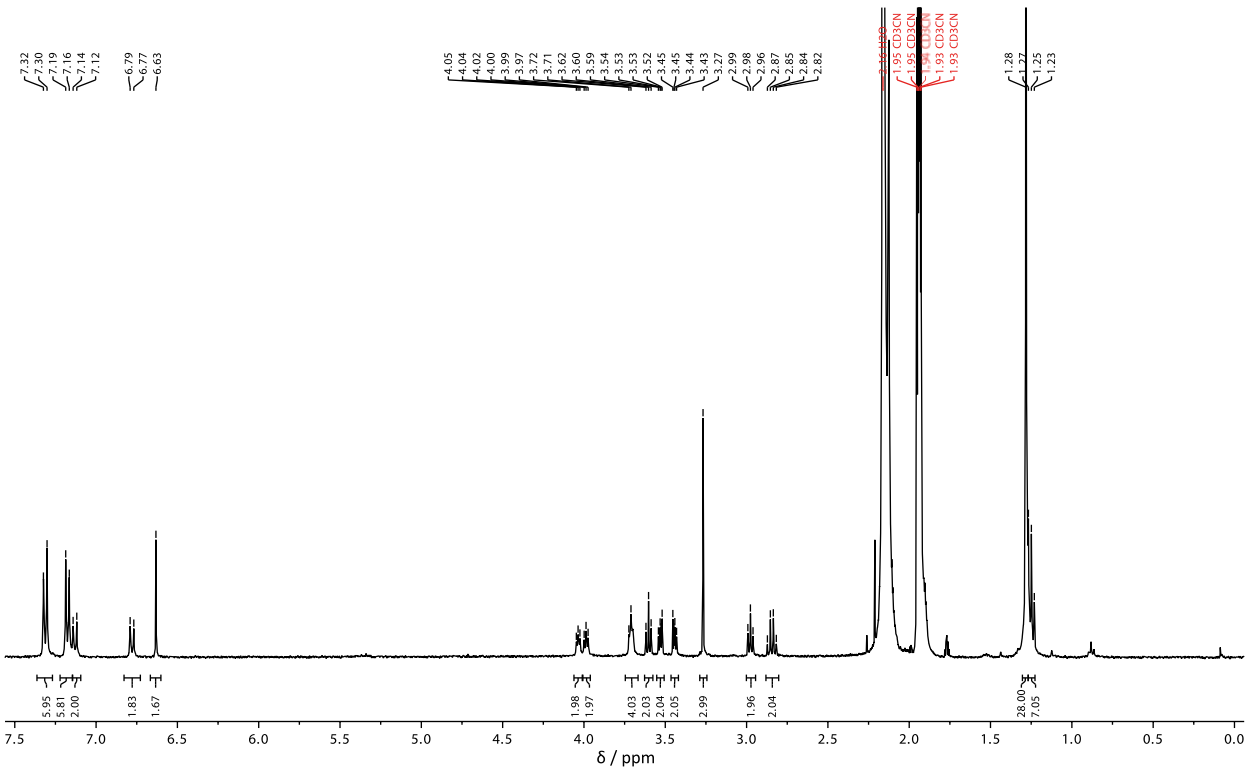

Fig. S16 ^{1}H NMR spectrum (400 MHz, 298K, CD_3CN) of the dumbbell **6**.

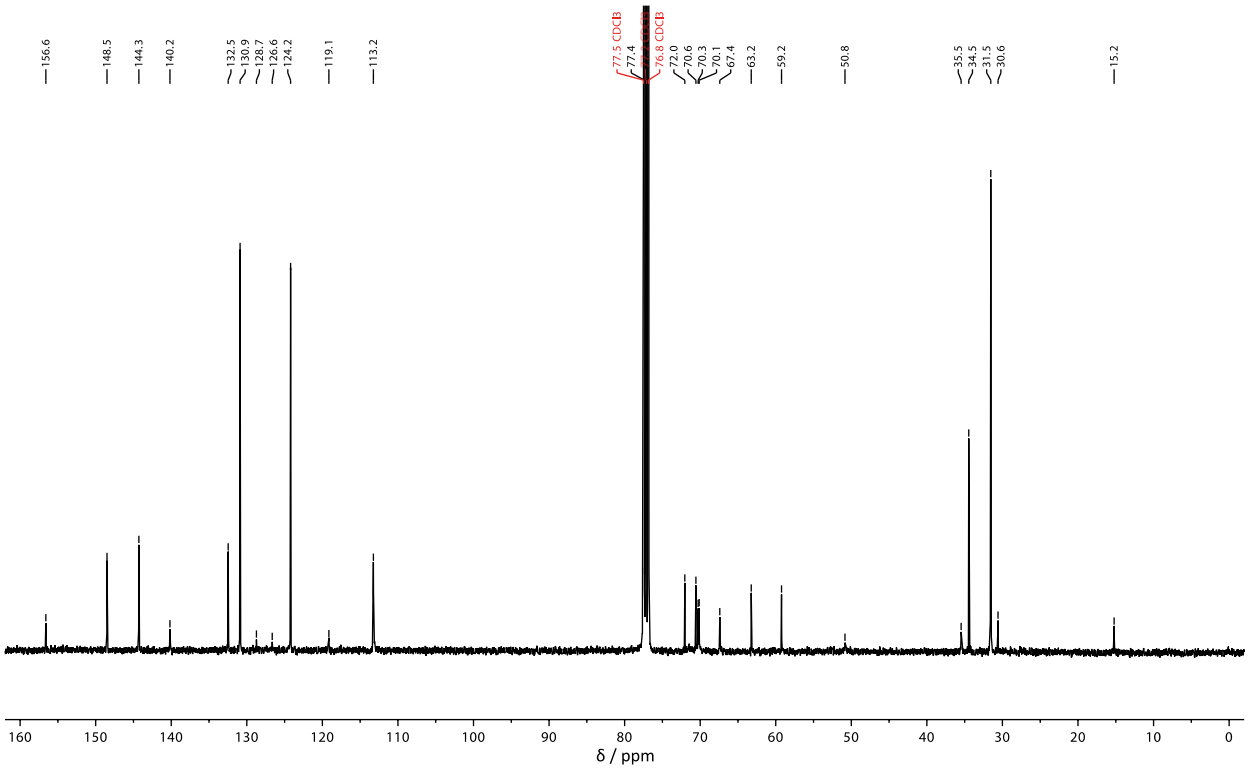

Fig. S17 **^{13}C NMR spectrum (100 MHz, 298K, $CDCl_3$) of** the dumbbell **6**.

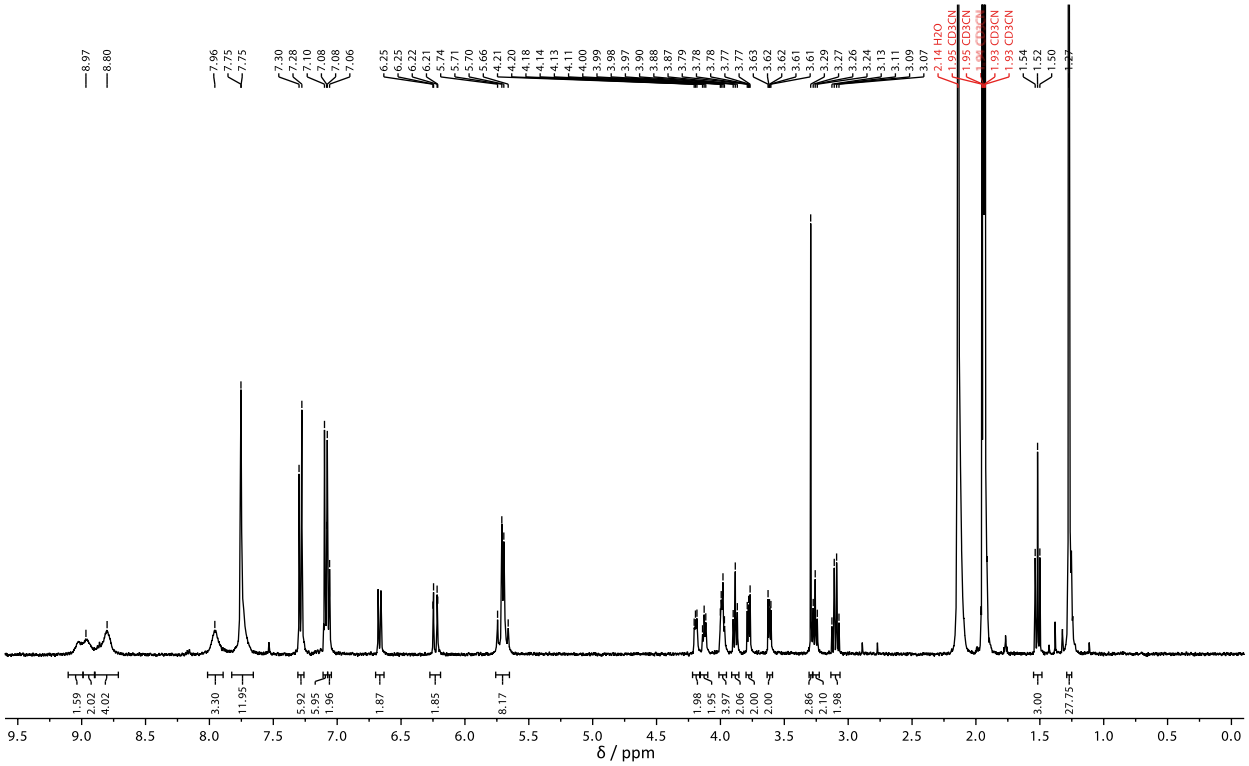

Fig. S18 ^{1}H NMR spectrum (400 MHz, 298K, CD_3CN) of the [2]rotaxane **2**•4PF_6.

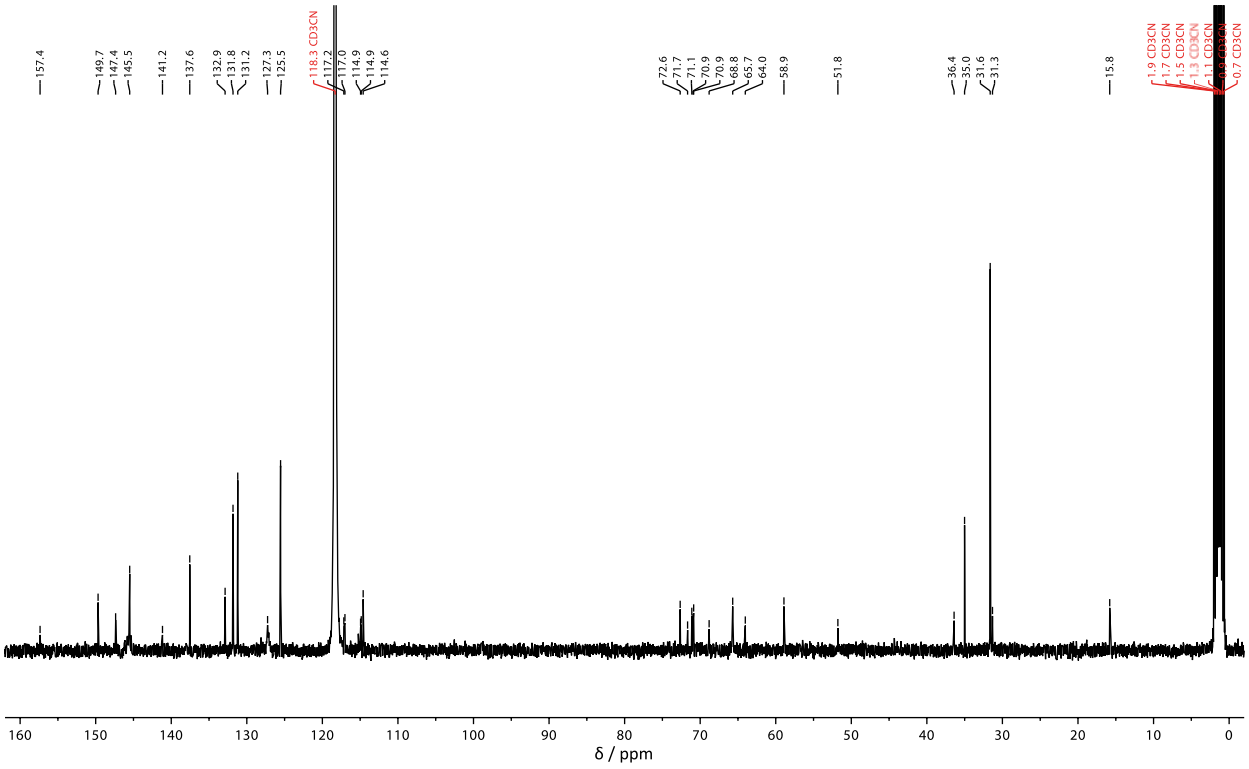

Fig. S19 ^{13}C NMR spectrum (100 MHz, 298K, CD_3CN) of the [2]rotaxane **2**•4PF_6.

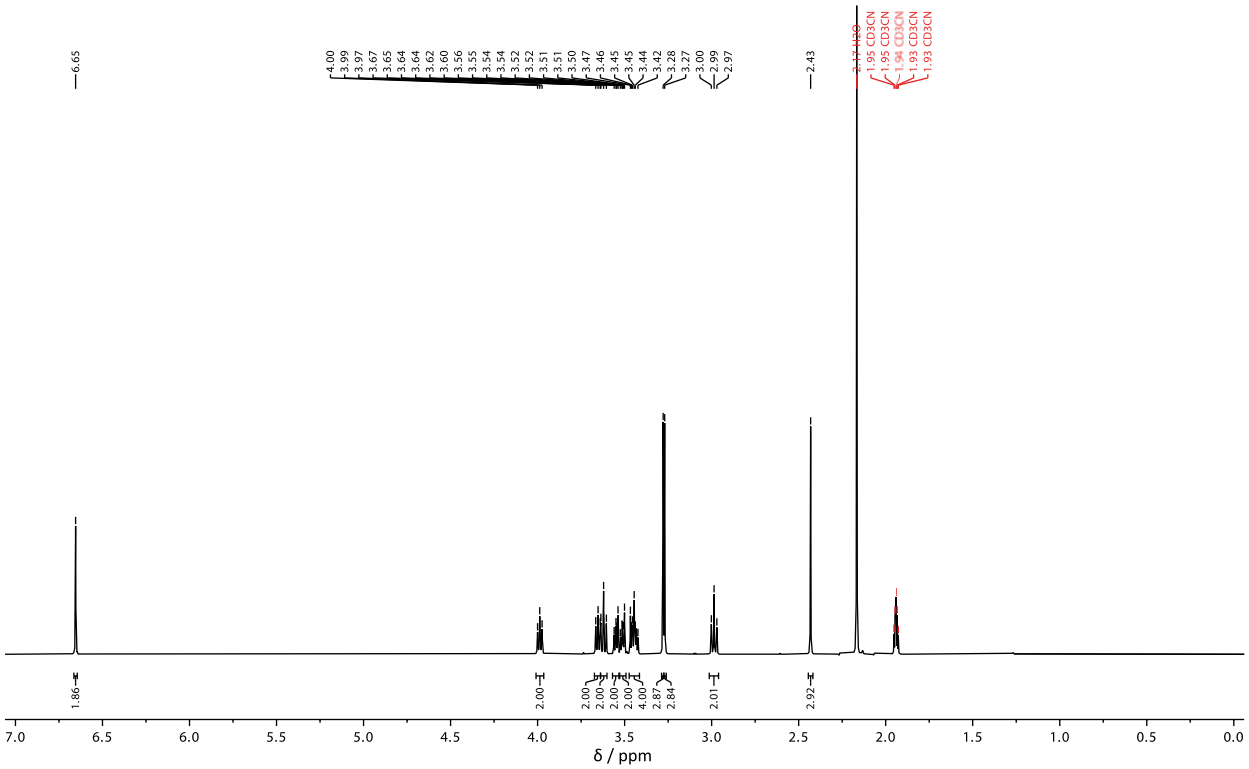

Fig. S20 ^{1}H NMR spectrum (400 MHz, 298K, CD_3CN) of the model compound **9**.

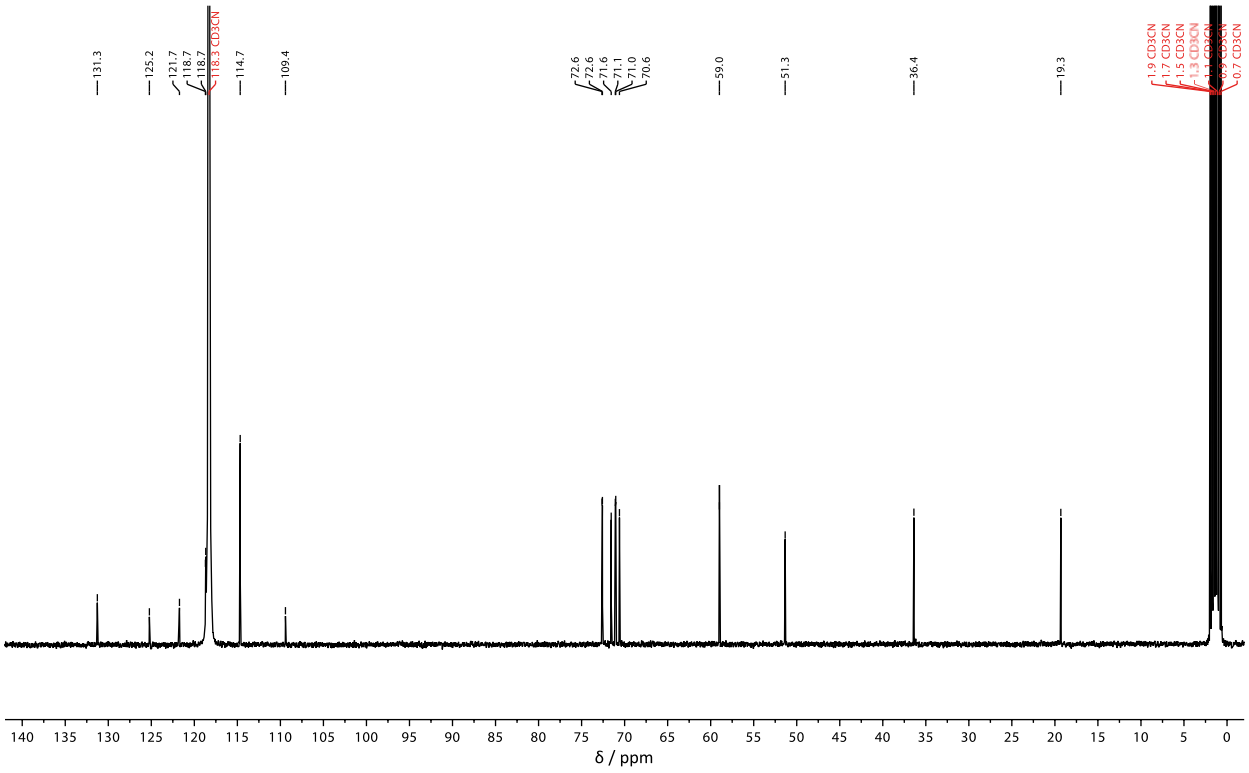

Fig. S21 ^{13}C NMR spectrum (100 MHz, 298K, CD_3CN) of the model compound **9**.

References

S1. M. Döbbelin, I. Azcune, M. Bedu, A. Ruiz De Luzuriaga, A. Genua, V. Jovanovski, G. Cabañero and I. Odriozola, *Chem. Mater.*, 2012, **24**, 1583–1590.

S2. A. Sørensen, S. S. Andersen, A. H. Flood and J. O. Jeppesen, *Chem. Commun.*, 2013, **49**, 5936–5938.

S3. S. Nygaard, C. N. Hansen and J. O. Jeppesen, *J. Org. Chem.*, 2007, **72**, 1617–1626.

S4. N. Koumura, E. M. Geertsema, M. B. van Gelder, A. Meetsma and B. L. Feringa, *J. Am. Chem. Soc.*, 2002, **124**, 5037–5051.